In Vivo MR Study of Brain Maturation in Normal Fetuses

Nadine Girard, Charles Raybaud, and Martine Poncet

PURPOSE: To illustrate normal maturation of the fetal brain, including the migrational layer, gray matter, early myelination of internal capsules, optic radiations, and corona radiata. **METHODS:** Seventy-seven fetal brains, ranging from 21 to 38 weeks of gestational age, were examined with MR in vivo; 33 were considered normal. MR examinations were performed as T1-weighted sequences in the axial, sagittal, and coronal planes. The neuropathologic examination (four cases) and clinical and/or neuroradiologic examinations confirmed the antenatal data. **RESULTS:** From 21 to 25 weeks, the cerebral ventricles are large, corresponding to the relative fetal hydrocephalus. A slight high signal intensity can be observed in the basal ganglia as early as 21 weeks. In the cerebral hemispheres, a multilayered pattern that can be observed from 23 to 28 weeks includes the cortical ribbon, the germinal matrix, and an intermediate layer corresponding to the migrating glial cells. These findings are probably related to areas of increased cellularity. A high signal intensity can be seen within the dorsal part of the brain stem as early as 23 weeks, within the posterior limb of the internal capsules at 31 weeks, and within the central area of the cerebral hemispheres at 35 weeks. Those patterns are probably caused by the evolving process of myelination. **CONCLUSIONS:** MR allows depiction of signal changes corresponding either to an increase in cellularity or to the evolving processes of myelination, depending on the stage of the pregnancy.

Index terms: Fetus, growth and development; Fetus, magnetic resonance; Brain, growth and development

AJNR Am J Neuroradiol 16:407–413, February 1995

The identification of criteria to assess the development of the brain could help in detecting early disturbances of fetal brain maturation. Fetal brain MR findings have been reported (1–17); normal fetal brain appearance in vivo has been observed in few cases (13, 14, 17). The purpose of this study is to report and illustrate the sequential changes in 33 cases of normal fetal brain maturation.

Patients and Methods

Thirty-three patients were examined. The stage of the pregnancy ranged from 21 to 38 weeks (Fig 1). In all cases, magnetic resonance (MR) imaging was performed to complement uncertain ultrasonographic data: "colpocephaly" in 14 cases, suspected microcephaly in 4 cases, choroid plexus cysts in 2 cases, oligohydramnios with intrauterine growth retardation in 4 cases, suspected dysraphism in 3 cases, suspected posterior fossa cyst in 1 case, suspected toxoplasmosis in 2 cases, and uterine malformation with twin pregnancy and death of the cotwin in 1 case. Therapeutic abortions were performed in 4 cases, either because of extracerebral malformations or chromosomal abnormalities. The neonate was stillborn in 2 cases. In these 6 cases, a neuropathologic examination was performed, and in 4 it confirmed that the brain was normal. In 27 other cases, clinical and/or neuroradiologic examinations (mainly ultrasonography) confirmed the antenatal findings.

In 30 cases, MR examinations were performed on a 1.0-T unit with spin-echo T1-weighted sequences (500–800/15[repetition time/echo time]); in 6 cases with turbo spin-echo T1-weighted sequences (1200–1300/19). Three early cases were investigated on a 0.5-T magnet. MR images were obtained in the coronal, axial, and sagittal fetal head planes. A long-repetition-time sequence was performed in 6 cases, using turbo spin-echo T2-weighted sequence (5000/160). MR studies were performed after percutaneous umbilical cord puncture, allowing fetal blood sampling and then curarization, except in 5 cases in which a fetal blood sample was not needed (4 cases) or the

Received January 5, 1994; accepted after revision June 16, 1994.

From the Hopital Nord, Neuroradiology, Marseille, France.

Address reprint requests to Prof. Charles Raybaud, Hopital Nord, Neuroradiology, Chemin des Bourrelly, 13326 Marseille Cedex 15, France

AJNR 16:407–413, Feb 1995 0195-6108/95/1602–0407

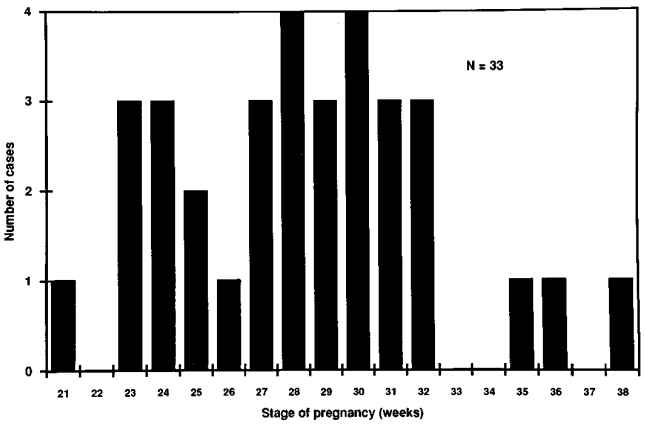

Fig 1. Normal fetal brain MR.

umbilical cord puncture could not be performed (1 case). Because ultrasound findings were abnormal, human-use committee permission was not needed. The fetus was in breech position in 5 cases, in transverse-lying position in 4 cases, and in cephalic position in the remaining cases. Motion artifacts related to the mother's respiratory or other movement or lack of curarization were observed in 5 cases. The MR images of the fetal brain were read according to the atlas of normal fetal brain morphology by Fees-Higgins and Larroche (18).

Results

In the young fetuses (21 to 25 weeks) the cerebral ventricles were large, corresponding to the relatively normal fetal "hydrocephalus" (Fig 2). Later on, the ventricles were smaller (Fig 3); at 25 weeks, they had become almost invisible (Fig 4). From 21 to 25 weeks, the brain was agyric, with undeveloped Sylvian fissures (Fig 1). Early gyral development could be observed as early as 27 weeks (Figs 3 and 5). It is noteworthy that the gyri were difficult to distinguish later on T1-weighted images, only because of the decrease in volume of the subarachnoid spaces.

A typical multilayered pattern was observed within the cerebral parenchyma from 23 to 28 weeks on T1-weighted images: the cortical ribbon, an intermediate layer (corresponding to the migrating glial cells), and the periventricular area (corresponding to the germinal matrix) were of high signal; the intermediate white matter layers were of a lower signal (Fig 2A). From 28 weeks on, the layered pattern became invisible, but the cortical ribbon appeared as a high signal (Fig 3), still allowing the differentiation

Fig 2. Week 23, morphology and myelination. Axial (*A* and *B*), sagittal (*C*), and coronal (*D*) spin-echo T1-weighted images (800/15/2 excitations; matrix, 190 × 256).

A, The ventricles and the subarachnoid spaces are large. The brain is agyric. The Sylvian fissures have not formed. A typical multilayered pattern is observed within the cerebral parenchyma. Diffuse high signal intensity is observed in the basal ganglia.

B, *C*, and *D*, High signal intensity is seen in the brain stem, sparing the anterior part of the pons (*arrow*).

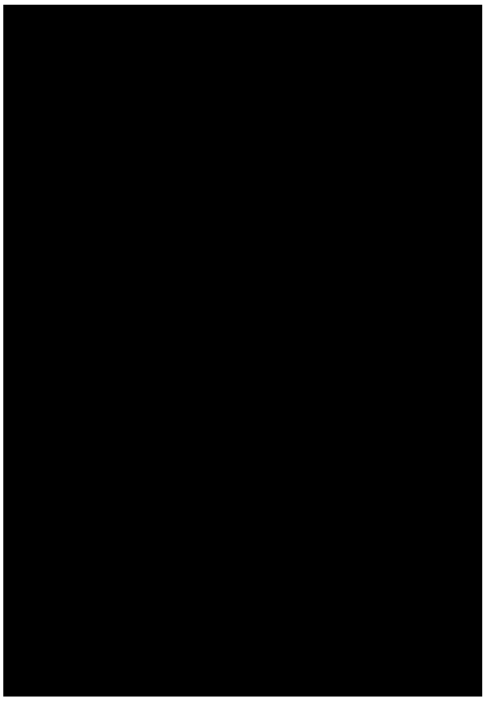

Fig 3. Week 29, morphology. Coronal spin-echo T1-weighted image (600/15/2, matrix, 190 × 256). Early gyral formation is observed (*white arrows*). The multilayered pattern is not visible, but the cortical ribbon appears still as a high signal (*black arrows*). The ventricles are small. Basal ganglia appear bright in the areas corresponding to the lenticular nucleus.

between the cortex and the white matter: the cerebral parenchyma was homogeneous with the loss of the multilayered pattern (Fig 4A). After 29 weeks and until the end of the pregnancy, the cortical ribbon was more difficult to identify on T1-weighted images; it was better depicted on T2-weighted images (Fig 6).

A diffuse high signal intensity could be observed in the basal ganglia as early as 21 weeks on T1-weighted images, and was still visible during the pregnancy (Fig 2A). A high signal intensity could be seen in the brain stem as early as at 23 weeks on T1-weighted images (Figs 2B, C, and D); it was mainly localized to the posterior part of the pons and medulla, corresponding to the sensory tracts; at 31 weeks, it reached the midbrain. A localized high signal could be observed on T1-weighted images in the posterior limbs of the internal capsules as early as at 31 weeks (Fig 7), then in the optic radiations at 35 weeks (Fig 4B), and in the subcortical white matter corresponding to the central area at 35 weeks (Fig 8). All of those signal changes are summarized in Figure 9.

Discussion

Ultrasonography has proved to be the method of choice for examination of the fetal brain in utero. However, MR can be used to investigate the fetal brain, usually when ultra-

Fig 4. Week 36, morphology and myelination.

A and *B*, Axial spin-echo T1-weighted images (700/15/2; matrix, 190 × 256). The ventricles are almost invisible. The gyri are difficult to distinguish because of the decrease in volume of the subarachnoid spaces. The parenchyma is homogeneous with loss of the multilayered pattern. Early myelination is observed within the internal capsules (*A*) and in the proximal optic radiations (*B*) (*arrows*). Mesencephalon and basal ganglia appear bright (*B*).

Fig 5. Week 28, morphology. Axial turbo spin-echo T2-weighted images (5000/160/1; matrix, 234 × 256).

A (*thin arrows*), Early gyral formation is observed. Cortical ribbon appears as a low signal compared with white matter and subarachnoid spaces, which appear bright (*thick arrow*).

B, Note that basal ganglia, mesencephalon, and superior cerebellar peduncles appear as low signal.

sonographic examination is inconclusive or inadequate. MR seems to be more efficient than ultrasound in evaluating ventricular walls and subarachnoid spaces, and particularly in demonstrating intraparenchymal tissue organization. Moreover, clastic lesions (ie, atrophy, porencephaly) are very difficult to depict with ultrasound; in those cases, MR may be helpful in defining such lesions.

Our series of 33 cases showed the morphological changes of the fetal brain and the change of signals between gray and white matter. Some studies have already described MR of

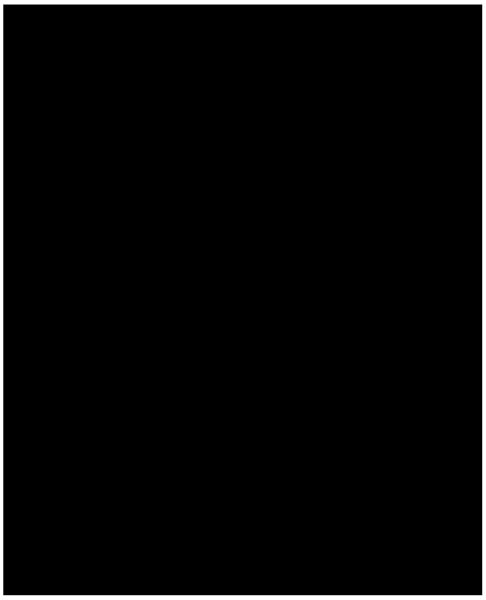

Fig 6. Week 32, morphology. Axial turbo spin-echo T2-weighted image (5000/160/1; matrix, 234 × 256). Cortical ribbon is well delineated from subarachnoid spaces and white matter. Note that external capsules appear bright.

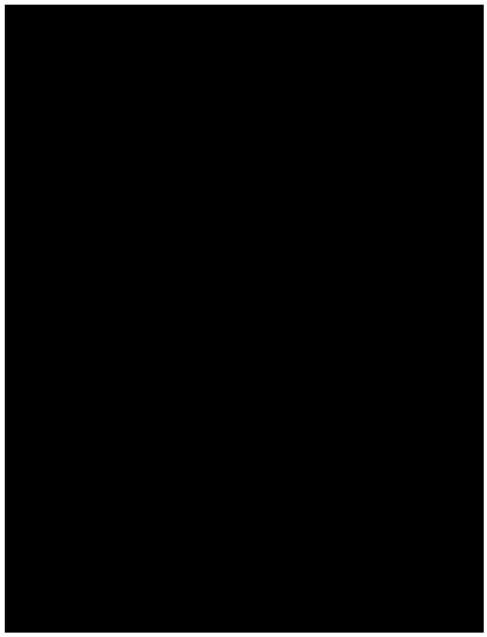

Fig 7. Week 32, myelination. Axial turbo spin-echo T1-weighted image (1200/19/2; matrix, 256 × 256). Early myelination is observed in the posterior limbs of the internal capsules (*arrow*). It is better depicted on the left side because the fetal head is not straight.

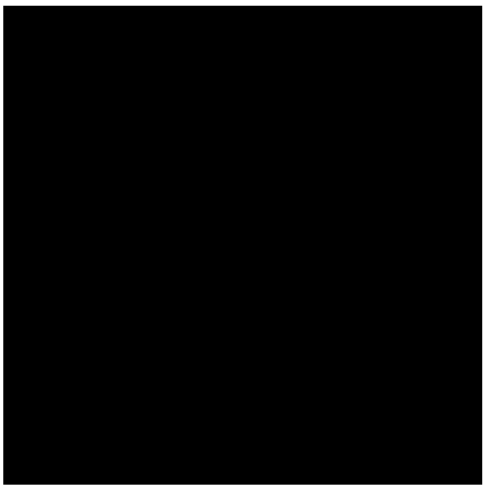

Fig 8. Week 35, myelination. Parasagittal spin-echo T1-weighted image (700/15/2; matrix, 190 × 256). Early myelination is observed within the subcortical white matter corresponding to the central area (*arrow*). Posterior limb of the internal capsule is also seen (*thick arrow*).

the fetal brain (1–17); a few were concerned with the normal fetal brain (13, 14, 17). Our study shows sequential signal changes on T1-weighted images within the brain stem, the basal ganglia, and the cerebral parenchyma in relation to the stage of the pregnancy.

The development of the central nervous system during intrauterine life is the result of morphological changes and maturation (including histogenesis and myelination) (19–33). Usually, myelination is considered to be a late process, beginning during the second half of the pregnancy and continuing during the first years of life (19, 27, 28). Microscopic myelination is already detectable at 20 weeks in the medial longitudinal fasciculus of the medulla and pons (33).

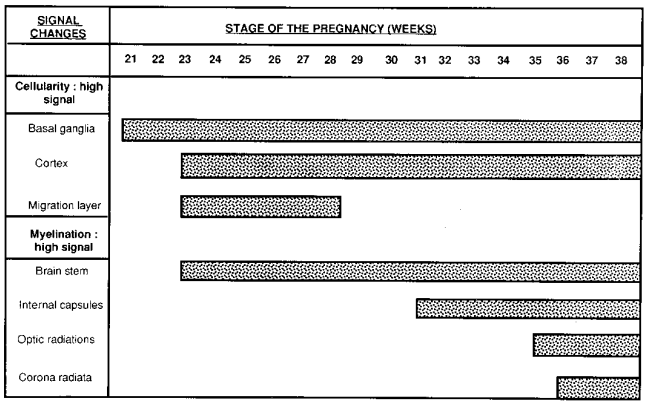

Fig 9. Signal changes of the developing fetal brain.

Histogenesis includes neurogenesis and gliogenesis. From 7 to 20 weeks, the neuroblasts migrate from the germinal matrix toward the surface of the brain; at 20 weeks, the six-layered cortex is fully achieved. From 20 weeks on, the glial cells develop to form astroglia and ologodendroglia (the so-called myelination gliosis). The migrating glial cells form an intermediate layer within the white matter. A postnatal MR study of brain myelination has been reported (34–43). In those studies, T1-weighted sequences show the "myelination gliosis" as a high signal extending into the white matter; T2-weighted sequences show the myelination proper, which appears as a low signal intensity (43). High signal intensity on the T1-weighted sequences is correlated with the evolving myelination either because of the accumulation of lipidic precursors of myelin, or because of the phenomenon of magnetization transfer (34).

The multilayered pattern of the cerebral hemispheres has been reported in a 23-week-old fetus (13) and in a 24-week-old premature fetus (17). In our study, that typical pattern can be observed from 23 to 28 weeks of gestational age. According to the histopathologic data taken from the literature (18), the high signal intensity observed within the cortical ribbon, the intermediate layer, the germinal matrix, and the basal ganglia is related to the high cellularity in those areas at 23 weeks. The multilayered pattern within the cerebral hemisphere is only temporary; after 28 weeks, the parenchyma becomes homogeneous and slightly hypointense on T1-weighted images, with the high signal of the cortical ribbon still persisting until the end of the pregnancy. The cortical ribbon is more difficult to identify after 29 weeks with T1-weighted sequences only, probably because of the decrease in volume of the subarachnoid spaces. On the other hand, T2-weighted images allow the differentiation of cortex and white matter until the end of pregnancy. Although the layered pattern of the cerebral hemispheres is well correlated with the cellularity by histopathologic studies (18), the homogeneous appearance of white matter that develops after 28 weeks on T1-weighted images is not clearly explained. However, two factors may account for this: *(a)* the germinal matrix becomes thinner, with a rarefaction of cells after 30 weeks (18, 24) and (*b*) the evolving processes of myelination begin within the white matter (30, 33), including accumulation of lipid and pro-

tein precursors and myelination gliosis, leading to an increase in cellular density throughout the white matter, and consequently an increase in signal on the MR images. From a histologic point of view, microscopic myelination is present at 27 to 28 weeks in the central part of the corona radiata. Furthermore, at the same time, histologic data (44) show that from 28 weeks of gestational age on, a decrease in cellular packing density can be observed within the cortex: therefore, the global signal intensity of the future white matter approaches the cortical signal. The cortical ribbon, however, appears as high signal when compared with the underlying white matter until the end of the pregnancy, but it becomes less apparent because its relative thickness is reduced from the preceding weeks.

As early as at 21 weeks, a high signal intensity could be observed in the basal ganglia on T1-weighted images. According to histologic data (18), it is related to an increase in cellularity, because myelination appears later, at 28 weeks (27). From 23 weeks on, a high signal intensity can be detected in the brain stem on T1-weighted images, predominantly dorsally, corresponding to the sensory tracts. It can be related to the evolving processes of myelination, according to the histopathologic studies (27, 28, 33) that show that oligodendrogliosis is present as early as at 22 weeks in the acoustic system of the brain stem (27, 28). Microscopic myelination is already present at 20 weeks in the medial longitudinal fasciculus of the medulla and pons, and at 23 weeks in the medial lemniscus (33). Later, histologically (33), myelination is present in the posterior limbs of the internal capsules at 32 weeks, at 34 weeks in the corticospinal tract of the mesencephalum, and at 38 weeks in the anterior limbs of the internal capsules and optic radiations. This explains the high signal intensity we observed in the posterior limbs of the internal capsules at 31 weeks, in the optic radiations, and in the subcortical white matter centrally at 35 weeks. Figure 9 summarizes the small changes related to cellularity and myelination of fetal brain.

In conclusion, MR is more sensitive than ultrasound in establishing criteria of normal signals of the developing fetal brain. Signal changes can be explained by several phenomena, including increase in cellularity, myelination gliosis, and myelination proper. Potential benefits of MR are: (*a*) recognition of disorders of the brain histogenesis beyond the scope of ultrasound as early as possible (for instance, micropolygyria has been observed histologically in fetuses 25 and 26 weeks old) and (*b*) follow-up of the fetal brain after a maternal injury (ie, monocarboxide poisoning; Figure 10).

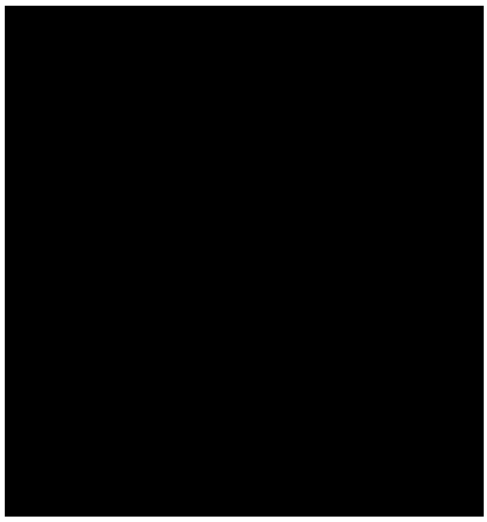

Fig 10. Week 32, monocarboxide poisoning. Axial turbo spin-echo T1-weighted image (1200/19/2; matrix, 256 × 256). Hypointensity is seen in the white matter of the frontal lobes (*arrows*). Normal high signal is not depicted in the posterior limbs of the internal capsules, probably because of delayed maturation.

References

1. Hill MC, Lande IM, Larsen JW. Prenatal diagnosis of fetal anomalies using ultrasound and MRI. *Radiol Clin North Am* 1988;26: 287–307
2. Lowe TW, Weinre J, Santos-Ramos R, Cunningham FG. Magnetic resonance imaging in human pregnancy. *Obstet Gynecol* 1985; 66:629–633
3. Weinreb JC, Lowe TW, Santos-Ramos R, Cunningham FG, Parkey R. Magnetic resonance imaging in obstetric diagnosis. *Radiology* 1985;154:157–161
4. McCarthy SM, Filly RA, Stark DD, et al. Obstetrical magnetic resonance imaging: fetal anatomy. *Radiology* 1985;154:427–432
5. Powell MC, Worthington BS, Buckley JM, Symonds EM. Magnetic resonance imaging (MRI) in obstetrics, II: fetal anatomy. *Br J Obstet Gynaecol* 1988;95:120–123
6. Smith IW, Adam AH, Philipps WDP. NMR imaging in pregnancy. *Lancet* 1983;i:61–62
7. Smith IW, Kent C, Abramovich DR, Sutherland HW. Nuclear magnetic imaging: a new look at the fetus. *Br J Obstetr Gynaecol* 1985;92:1024–1033
8. Weinreb JC, Lowe T, Cohen JM, Kutler M. Human fetal anatomy: MR imaging. *Radiology* 1985;157:715–720
9. Mattison DR, Angtuaco T. Magnetic resonance imaging in prenatal diagnosis. *Clin Obstet Gynecol* 1988;31:353–389
10. Aguirre Vila-Coro A, Dominguez R. Intrauterine diagnosis of hydranencephaly by magnetic resonance. *Magn Reson Imaging* 1989;7:105–107

11. Thickman D, Mintz M, Mennuti M, Kressel HY. MR imaging of cerebral abnormalities in utero. *J Comput Assist Tomogr* 1984;8: 1058–1061
12. Toma P, Lucigrai G, Ravegnani M, Cariati M, Magnano G, Lituania M. Hydrocephalus and porencephaly: prenatal diagnosis by ultrasonography and MR imaging. *J Comput Assist Tomogr* 1990;14: 843–845
13. Girard NJ, Raybaud CA. In vivo MRI of fetal brain cellular migration. *J Comput Assist Tomogr* 1992;2:265–267
14. Girard N, Raybaud C, D'Ercole C, et al. In vivo MR imaging of the fetal brain. *Neuroradiology* 1993;6:431–436
15. D'Ercole C, Girard N, Boubli L, et al. Prenatal diagnosis of fetal cerebral abnormalities by ultrasonography and magnetic resonance imaging. *Eur J Obstet Gynecol Reprod Biol* 1993;50:177–184
16. Hansen PE, Ballesteros MC, Soila K, Garcia L, Howard JM. MR imaging of the developing human brain: prenatal development. *Radiographics* 1993;13:21–26
17. Mintz MR, Grossman RI, Isaacson G, et al. MR imaging of fetal brain. *J Comput Assist Tomogr* 1987;11:120–123
18. Fees-Higgins A, Larroche JC. *Development of the Human Fetal Brain: An Anatomical Atlas*. Paris: Masson, 1987:13–189
19. Larroche JC. Development of the central nervous system. In: Larroche JC, ed. *Developmental Pathology of the Neonate*. Amsterdam: Elsevier/North-Holland Biomedical Press, 1977:319–353
20. Friede RL. Gross and microscopic development of the central nervous system. In: Friede RL, ed. *Developmental Neuropathology* Berlin: Springer-Verlag, 1989:2–20
21. Volpe JJ. Neuronal proliferation, migration, organization, and myelination. In: Volpe JJ, ed. *Neurology of the Newborn*. Philadelphia: WB Saunders Co, 1987:33–68
22. Roessmann U, Gambetti P. Astrocytes in the developing human brain. *Acta Neuropathol Beil* 1986;70:308–313
23. Langworthy OR. Development of behavior patterns and myelinization of the nervous system in the human fetus and infant. *Contrib Embryology* 1993;139;1–57
24. Smith JF. The development and maturation of the brain. In: Smith JF, ed. *Pediatric Neuropathology*. New York: McGraw-Hill Book Co, 1974:1–19
25. Larroche JC. The development of the central nervous system during intrauterine life. In: Falkner F, ed. *Human Development*. Philadelphia: WB Saunders Co, 1966:257–276
26. Larroche JC, Amakawa H. Glia of myelination and fat deposit during early myelinogenesis. *Biol Neonate* 1973;22:421–435
27. Yakovlev PI, Lecours A. The myelinogenetic cycles of regional maturation of the brain. In: Minkowski A, ed. *Regional Development of the Brain in Early Life*. Oxford: Blackwell Scientific Publications, 1967:3–70
28. Yakovlev PI. Morphological criteria of growth maturation of the nervous system in man. In: Kolb LC, Masland RL, Cooke RE, eds. "*Mental Retardation": Association for Research into Nervous and Mental Diseases*. Baltimore: Williams and Wilkins, 1962:1–46
29. Evrard P, Miladi N, Bonnier C, Gressens P. Normal and abnormal development of the brain. In: Rapin I, Segalowitz SJ, Boller F, Grafman J, eds. *Handbook of Neuropsychology*, vol 6: *Child Neuropsychology*. Amsterdam: Elsevier Science Publishers BV, 1992:11–44
30. Mickel HS, Gilles FH. Changes in glial cells during human telencephalic myelinogenesis. *Brain* 1970;93:337–346
31. Jammes JL, Gilles FH. Telencephalic development: matrix volume and isocortex and allocortex surface areas. In: Gilles FH, Leviton A, Dooling EC, eds. *The Developing Human Brain-Growth and Epidemiologic Neuropathology*. Boston: John Wright PSG Inc, 1983:59–86
32. Cooling EC, Chi JG, Gilles FH. Telencephalic development: changing gyral patterns. In: Gilles FH, Leviton A, Dooling EC, eds. *The Developing Human Brain-Growth and Epidemiologic Neuropathology*. Boston: John Wright PSG Inc, 1983:94–104
33. Gilles FH, Shankle W, Dooling EC. Myelinated tracts: growth patterns. In: Gilles FH, Leviton A, Dooling EC, eds. *The Developing Human Brain-Growth and Epidemiologic Neuropathology*. Boston: John Wright PSG Inc, 1983:117–183
34. Valk J, Van Der Knaap MS. Myelination and retarded myelination. In: Valk J, Van Der Knaap MS, eds. *Magnetic Resonance of Myelin, Myelination, and Myelin Disorders*. Berlin: Springer-Verlag, 1989:26–65
35. Barkovich A, Kyos BO, Jackson DE, Norman D. Normal maturation of the neonatal and infant brains: MR imaging at 1.5 T. *Radiology* 1988;166:173–180
36. Dietrich RB, Bradley WG, Zarogoza IV EJ, et al. MR evaluation of early myelination patterns in normal and developmentally delayed infants. *AJNR Am J Neuroradiol* 1988;9:69–76
37. Holland BA, Haas DK, Norman D, Brant Zawadzki M, Newton TH. MRI of normal brain maturation. *AJNR Am J Neuroradiol* 1986; 7:201–208
38. Holmes GL. Morphological and physiological maturation of the brain in the neonate and young child. *J Clin Neurophysiol* 1986; 3:209–238
39. Nowell MA, Hackney DB, Zimmerman RA, Bilaniuk LT, Grossman RI, Goldberg HI. Immature brain: spin echo pulse sequence parameters for high contrast MR imaging. *Radiology* 1987;162:272–273
40. Martin E, Kikinis R, Zuerrer M, et al. Developmental stages of human brain: an MR study. *J Comput Assist Tomogr* 1988;12: 917–922
41. McArdle CB, Richardson CJ, Nicholas DA, Mirfakhraee M, Hayden CK, Amparo EG. Developmental features of the neonatal brains: MR imaging, I: gray-white matter differentiation and myelination. *Radiology* 1987;162:223–229
42. Lee BCP, Lipper E, Nass R, Ehrlich ME, De Ciccio-Bloom E, Auld Pam. MRI of the central nervous system in neonates and young children. *AJNR Am J Neuroradiol* 1986;7:6055–616
43. Girard N, Raybaud C, Du Lac P. MRI study of brain myelination. *J Neuroradiol* 1991;18:291–307
44. Huttenlocher PR. Morphometric study of human cerebral cortex development. *Neuropsychologia* 1990;6:517–527

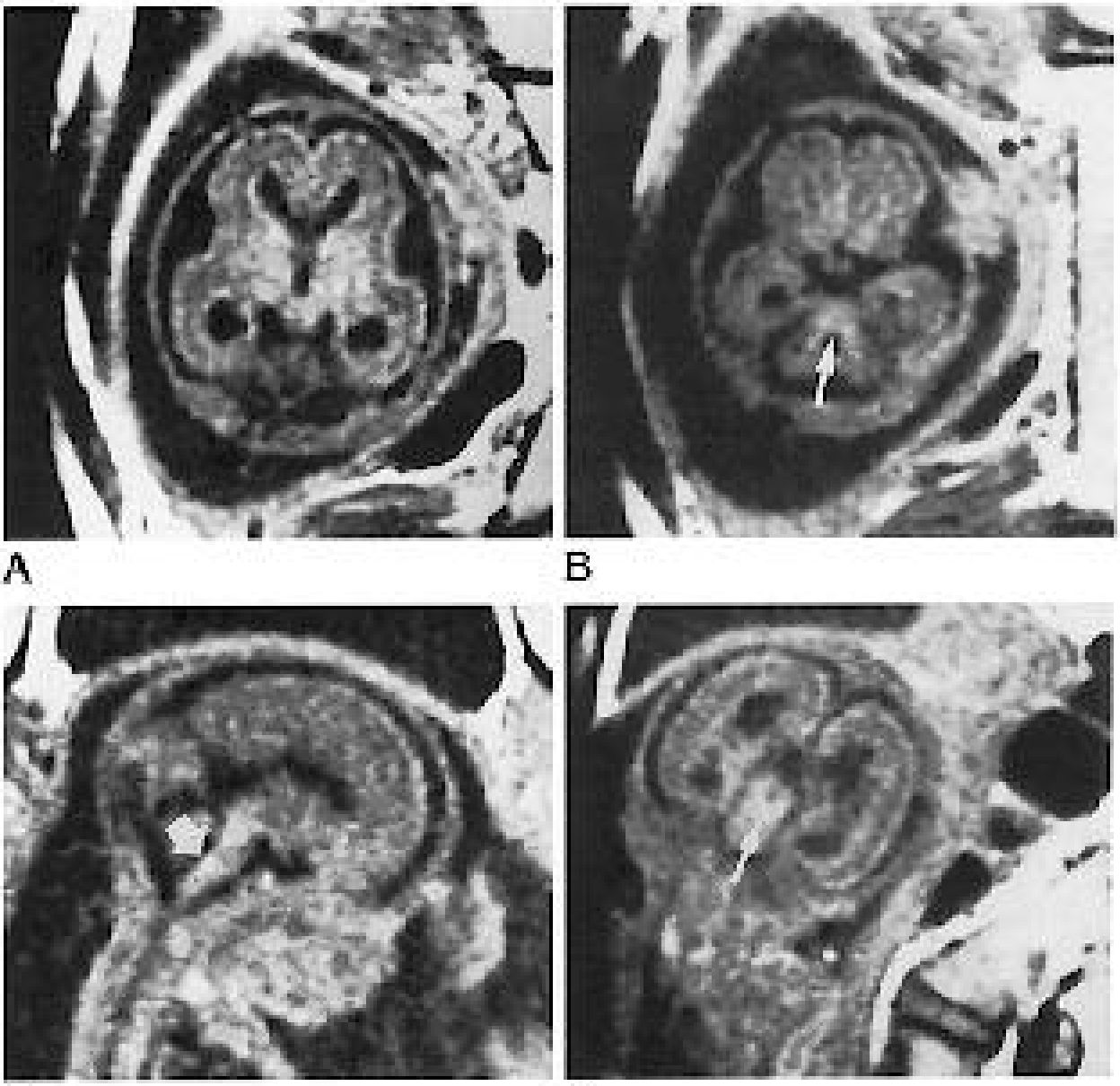
A
B
C
D

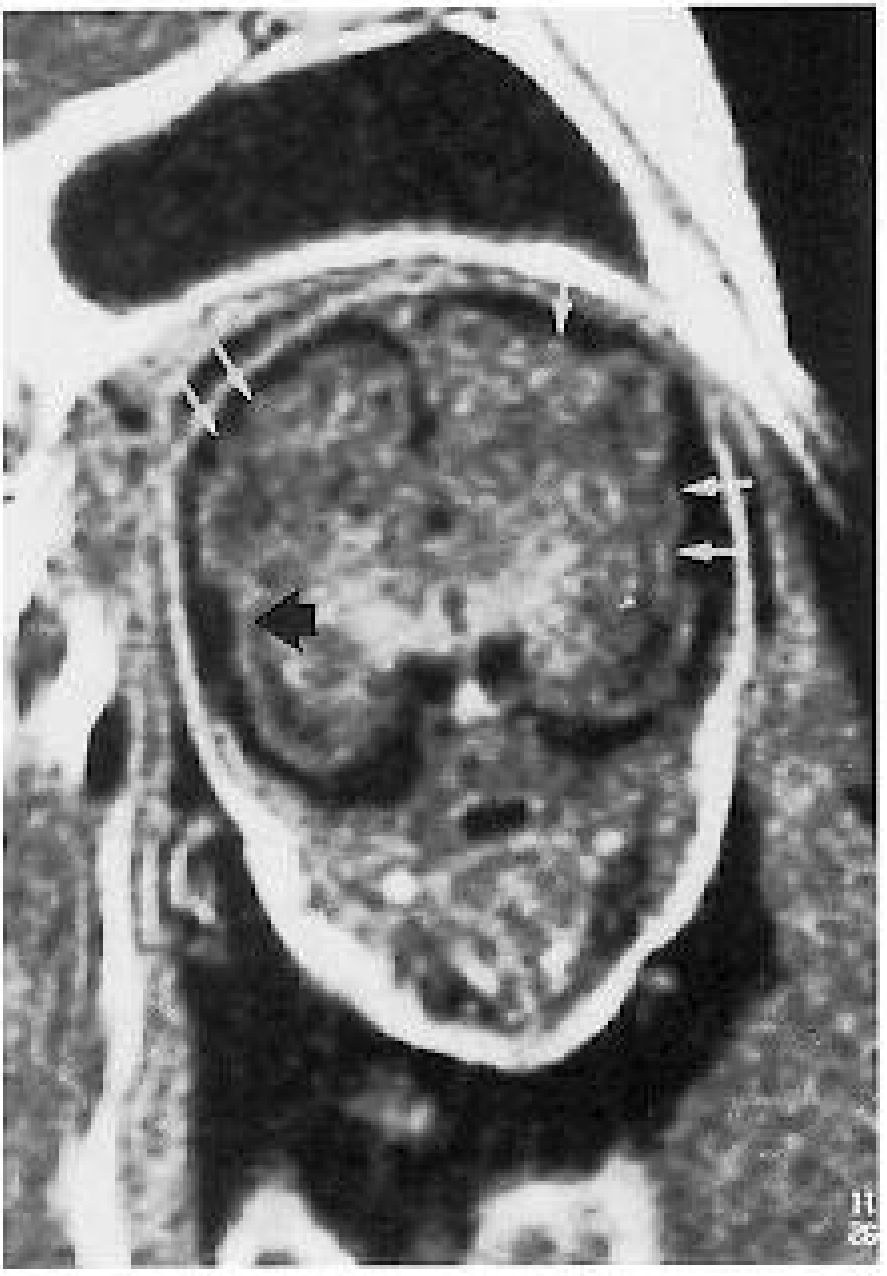

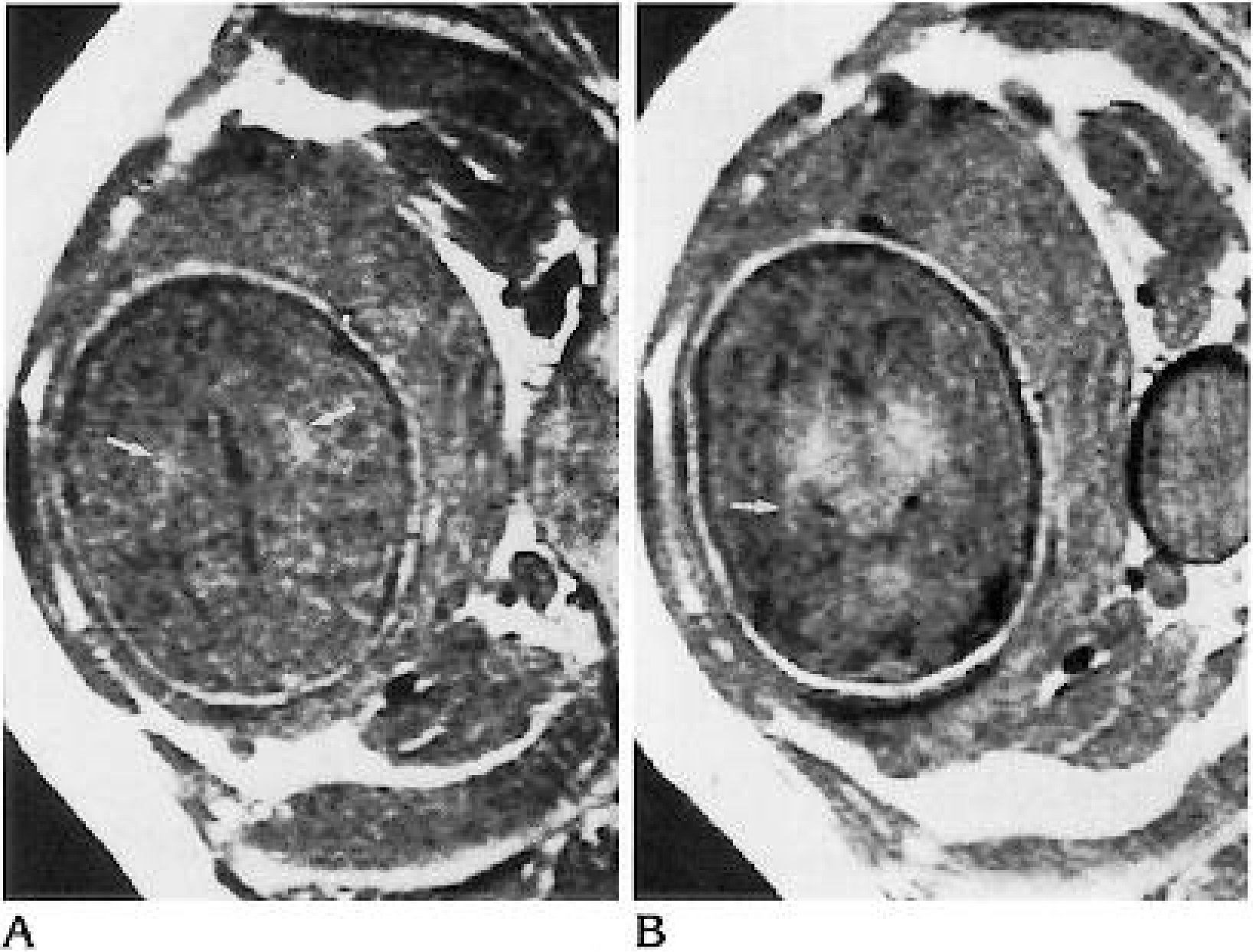
A
B

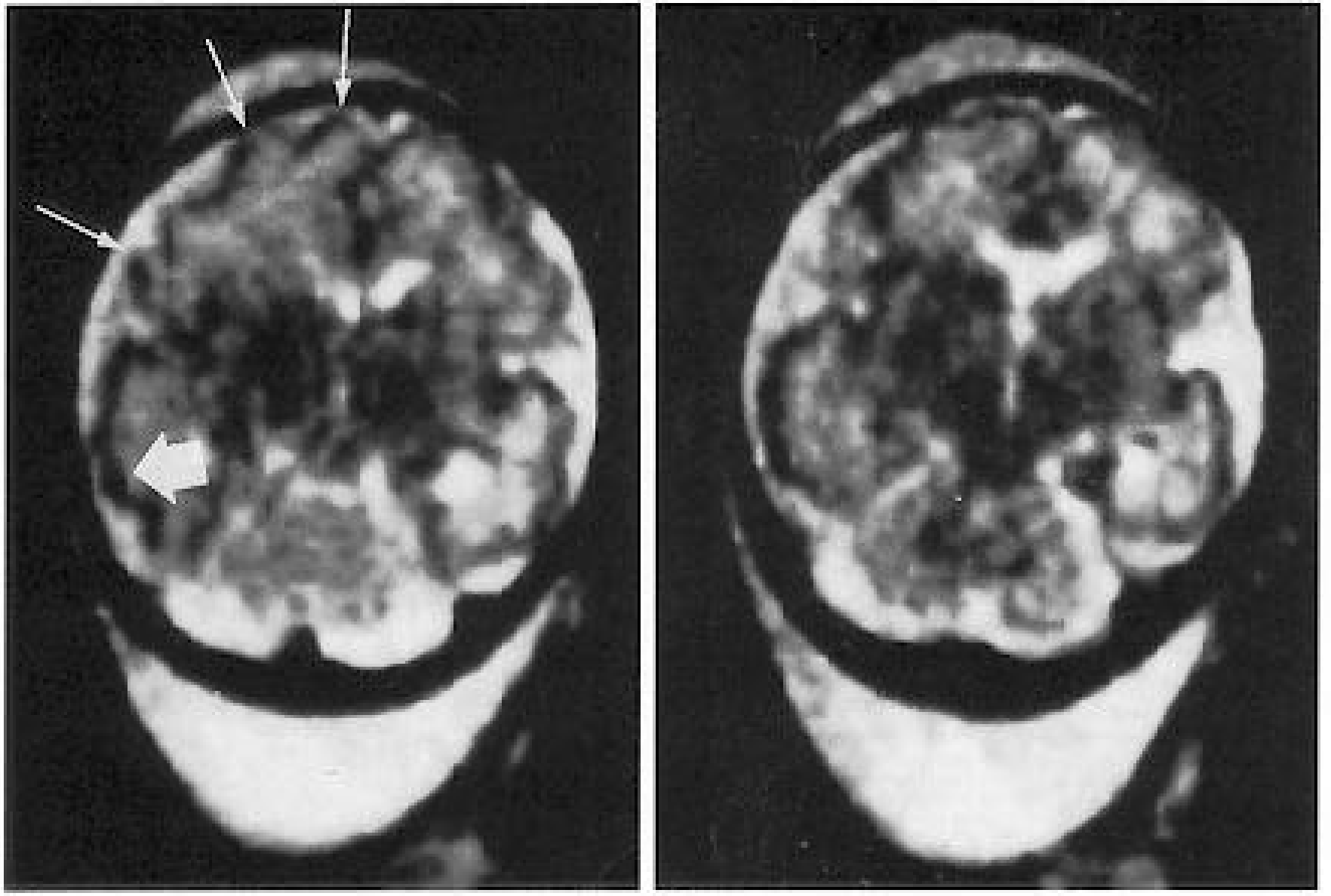
A
B